Dalton Transactions

Diamagnetic Molybdenum Nitride Complexes Supported by Diligating Tripodal Triamido-phosphine Ligands as Precursors to Paramagnetic Phosphine Donors

Journal:	*Dalton Transactions*
Manuscript ID:	DT-ART-04-2015-001415.R2
Article Type:	Paper
Date Submitted by the Author:	20-Jul-2015
Complete List of Authors:	Hatnean, Jillian; University of Windsor, Department of Chemistry & Biochemistry Johnson, Samuel; University of Windsor, Department of Chemistry and Biochemistry

TABLE OF CONTENTS GRAPHIC

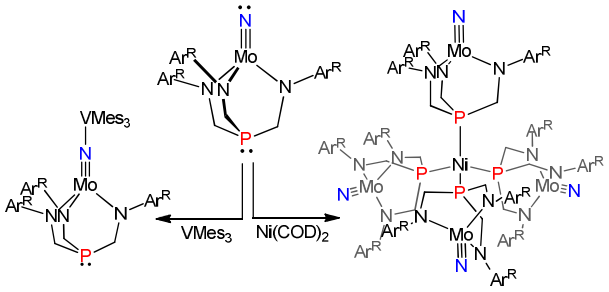

Complexes of the type $P(CH_2NAr^R)_3Mo{\equiv}N$ act as ditopic ligands that allow for the facile assembly of polymetallic complexes.

Diamagnetic Molybdenum Nitride Complexes Supported by Diligating Tripodal Triamido-phosphine Ligands as Precursors to Paramagnetic Phosphine Donors.

Jillian A. Hatnean, *Samuel A. Johnson*[*]

[†]Department of Chemistry and Biochemistry, University of Windsor 401 Sunset Avenue, Windsor, ON, Canada, N9B 3P4

Fax: (+1) 519-973-7098

E-mail: sjohnson@uwindsor.ca

Abstract

The reaction of the ligand precursors $P[CH_2NHAr^R]_3$ (**1a-c**) where Ar^R = 3,5-$(CH_3)_2$-C_6H_3 (**a**), Ph (**b**), and 3,5-$(CF_3)_2$-C_6H_3 (**c**), with $(Me_2N)_3Mo{\equiv}N$ generated the complexes $P(CH_2NAr^R)_3Mo{\equiv}N$ (**2a-c**). Complex **2c** was obtained in poor yield, due to the formation of $P(CH_2N\text{-}3,5\text{-}(CF_3)_2C_6H_3)_2(CH_2NH\text{-}3,5\text{-}(CF_3)_2C_6H_3)(NMe_2H)(NMe_2)Mo{\equiv}N$ (**3**) as the major product. Reaction of **2a-b** with $VMes_3THF$ generated the paramagnetic complexes $P(CH_2NAr^R)_3Mo(\mu\text{-}N)V(Mes)_3$ (**4a-b**). The reaction of **2a-b** with $Ni(acac)_2$ generated the Ni(0) complexes $Ni[P(CH_2NAr^R)_3Mo{\equiv}N]_4$ (**5a-b**) in poor yield. These complexes were synthesized in higher yields from the reaction of **2a-b** with $Ni(COD)_2$, where COD = 1,5-cyclooctadiene. Reaction of either **5a** with $V(Mes)_3THF$ or **4a** with $Ni(COD)_2$ generated the paramagnetic nonanuclear complex $Ni[P(CH_2NAr^R)_3Mo(\mu\text{-}N)VMes_3]_4$ (**6a**).

Cooperative effects between metals can lead to novel or increased reactivities and enhanced physical properties.[1] The search for cooperativity between metal centres has spurred chemists to find rational methods for the syntheses of binuclear and polymetallic clusters.[2] In the past, we have utilized triamidophosphine ligands of the type $P(CH_2NAr^R)_3$ for the assembly of binuclear complexes[3] and clusters,[4] where Ar^R is typically an aromatic substituent. Related ditopic ligands that are sometimes named Janus head ligands have become increasingly studied.[5] When bound to high oxidation state early transition metals, labeled M^1 in Scheme 1, the $P(CH_2NAr^R)_3$ ligands chelate using the hard amido donors similar to related claw-like ligands,[6] leaving the phosphine donor lone pair directed away from the metal centre, and available to bind to a second metal, labeled M^2 in Scheme 1.

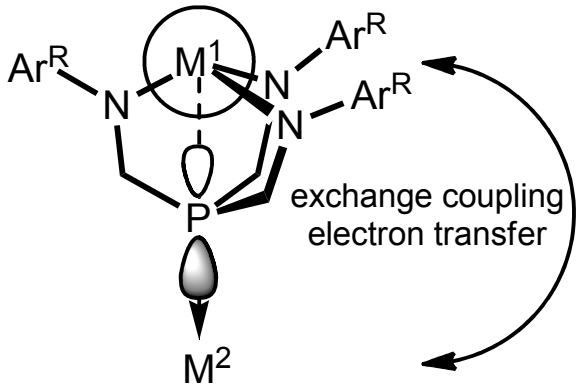

Scheme 1.

Although no formal bonding interaction occurs between M^1 and phosphine in these dinuclear complexes, the close proximity of the phosphine donor has several effects, which includes a decrease in the donor ability of the phosphine.[3a] We have previously shown how the appropriate choice of metals allows for through-space spin-exchange coupling between M^1 and

M^2.[3b] Similarly, electron transfer between M^1 and M^2 might allow for biomimetic catalytic chemistry and catalysis with redox steps, as the additional metals might readily shuttle electrons to the site of reactivity. For these reasons we have been interested in using these ligands to support low oxidation state early metals in the M^1 site.

We have previously investigated high-valent Al, Ti, Zr, Ta, Y and Gd with these $P(CH_2NAr^R)_3$ ligands,[3a, 7] as well complexes of Mg(II), Mn(II), and Cu(I).[4, 8] The target compounds $P(CH_2NAr^R)_3Mo{\equiv}N$ were attractive due to the many oxidation states available to Mo, and because of the ditopic nature of this molecule, where both functionalization at the phosphine donor and nitride moiety were possible. The chemistry of the mononuclear molybdenum complexes were also of interest. Group six transition metal nitrides participate in catalytic transformations, such as N-atom transfer reactions,[9] and nitrile-alkyne cross-metathesis to produce new transition metal alkylidynes.[10] Nitrido complexes are also products of dinitrogen cleavage.[9d, 11] Several computational studies have examined the reactivity of related group six nitride complexes.[11a, 12] Cummins *et al.* has already shown that capping molybdenum nitrides with an external molecule is a facile process, having synthesized a series of Lewis acid adducts and cationic complexes,[13] as well as capping with a second Mo moiety.[9b] Herein we describe the synthesis of complexes of the type $P(CH_2NAr^R)_3Mo{\equiv}N$ and an investigation into their reactivity as ditopic ligands.

Results and Discussion.

Synthesis of diamagnetic molybdenum nitrides. The syntheses of molybdenum nitride complexes using the ligand precursors $P(CH_2NH\text{-}3,5\text{-}(CH_3)_2C_6H_3)_3$ (**1a**) and $P(CH_2NHPh)_3$ (**1b**) was facile. The reaction of **1a** with $(Me_2N)_3Mo{\equiv}N$ in toluene produced $P(CH_2N\text{-}3,5\text{-}$

$(CH_3)_2C_6H_3)_3)_3Mo{\equiv}N$ (**2a**) as a red-orange precipitate over 12 h, as shown in eq 1. Similarly, the overnight reaction of **1b** with $(Me_2N)_3Mo{\equiv}N$ in toluene produced $P(CH_2NPh)_3Mo{\equiv}N$ (**2b**) as a dark orange precipitate. Analyses of the crude reaction mixtures by ^1H and $^{31}P\{^1H\}$ NMR spectroscopy revealed no significant side products were formed.

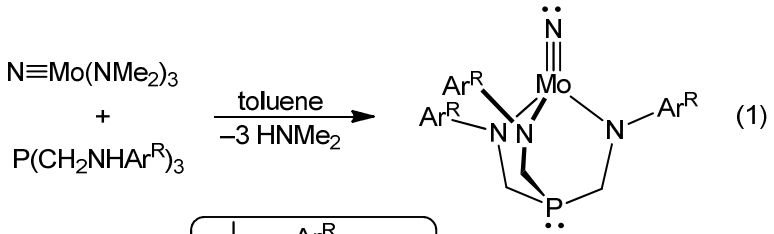

1a–b

	Ar^R
1a	3,5-$(CH_3)_2C_6H_3$
1b	Ph

2a–b

Compounds **2a** and **2b** both yielded X-ray quality crystals from slow evaporation of the reaction mixture at room temperature, and an ORTEP of the solid-state molecular structure of **2a** is shown in Figure 1. The complexes have no crystallographically imposed symmetry, but are approximately C_3 symmetric, with a propeller orientation of the aromatic amido substituents. The chelating ligand is bound through the amido donors with an average Mo–N length of 1.957(2) Å. The molybdenum-nitrogen triple bond length of 1.650(2) Å is in agreement with values reported in the CCSD for analogous molybdenum nitrides.[11d, 14] The geometry about the molybdenum center is pseudo-tetrahedral with the angles between amido donors smaller than 109.5 °. The N–Mo–N angles between the terminal nitrido and amido donors range from 110.83(9) to 113.14(10) °, also consistent with a tetrahedral geometry. These N≡Mo–N angles may indicate strain imposed by the ancillary ligand, because related complexes such as $(Ph_2N)_3Mo{\equiv}N$[14b] more commonly feature smaller N≡Mo– N angles in the range of 100-104 °.[11c, d, 14a, 14c] The lone pair on the phosphorus atom in **2a** is directed away from the molybdenum centre.[3b] Despite this, the chelating nature of the ligand retains an unusually short Mo(1)···P(1) distance of 2.965(1) Å.

Although this is longer than the mean reported Mo–P distance reported in the CCSD of 2.511 Å, it is comparable to some of the longer Mo-P bonding interactions, with examples up to 3.064(4) Å.[15] The sum of C–P–C angles is 311.68(2) °, which is close to the sum of angles of 311.4(1) observed in the related complex $P(CH_2NPh)_3Ti–NMe_2$, but less than the 315.0(2) sum of angles observed in $P(CH_2NPh)_3Ta=N^tBu$. In all these examples, the C–P–C angles increase from the ligand precursors, so that the chelate can accommodate the metal centre. The solid-state structure of complex **2b** determined by X-ray crystallography displays similar connectivity, bond lengths. Full structural details are provided in the Supporting Information.

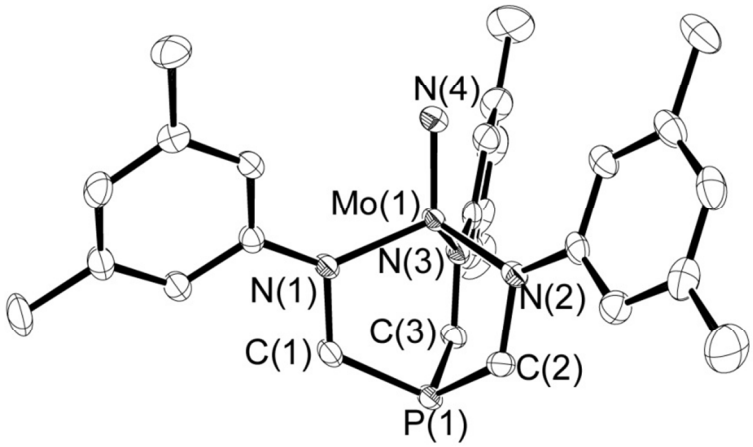

Figure 1. ORTEP of the solid-state molecular structure of **2a** as determined by X-ray crystallography. Hydrogen atoms omitted for clarity. Selected bond lengths or distances (Å): Mo(1)–N(4), 1.650(2); Mo(1)–N(1), 1.958(2); Mo(1)–N(2), 1.956(2); Mo(1)–N(3), 1.959(2); Mo(1)···P(1), 2.965(1). Selected angles in degrees: N(4)–Mo(1)–N(1), 110.83(9); N(4)–Mo(1)–N(2), 111.69(10); N(4)–Mo(1)–N(3), 113.14(10); N(1)–Mo(1)–N(2), 104.77(8); N(1)–Mo(1)–N(3), 108.13(8); N(2)–Mo(1)–N(3), 107.88(8).

The reaction of the ligand precursor $P(CH_2NH\text{-}3,5\text{-}(CF_3)_2C_6H_3)_3$ (**1c**) with $(Me_2N)_3Mo{\equiv}N$ in toluene overnight unexpectedly yielded two products, a dark red crystalline material identified as $P(CH_2N\text{-}3,5\text{-}(CF_3)_2C_6H_3)_2(CH_2NH\text{-}3,5\text{-}(CF_3)_2C_6H_3)(NMe_2H)(NMe_2)Mo{\equiv}N$ (**3**), where only two ligand arms are attached to the Mo centre and a bound NMe_2H moiety remains, and $P(CH_2N\text{-}3,5\text{-}(CF_3)_2C_6H_3)_3Mo{\equiv}N$ (**2c**) as a brown powder in a 5 : 1 mixture, as shown in eq 2.

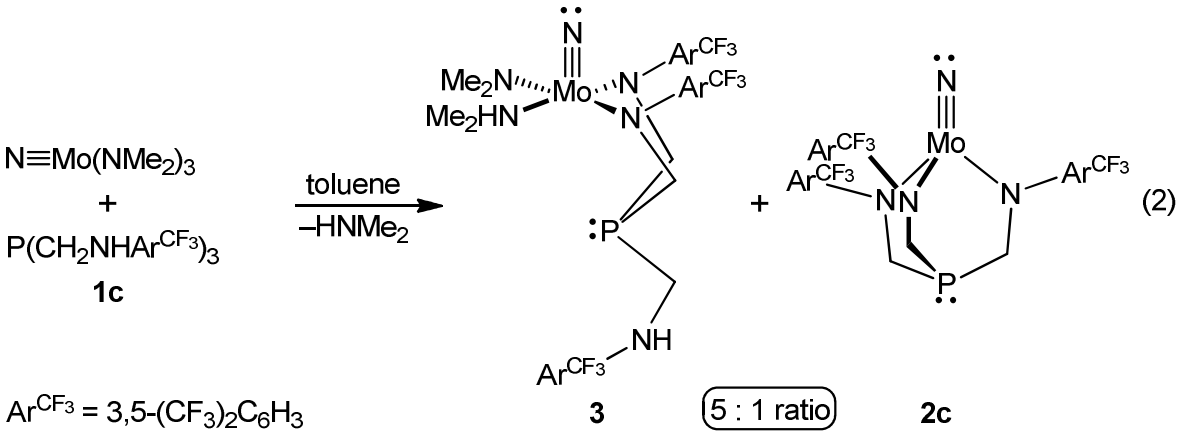

The red precipitate of **3** yielded crystals that were suitable for X-ray crystallography, and an ORTEP of the solid-state molecular structure is shown in Figure 2. The complex crystallized with an equivalent of toluene disordered over two sites. The ligand moiety shows only two arms bound through the amido donors to the molybdenum center, while the third arm is distant from the metal centre. The metal centre retains a bound NMe_2 ligand, as well as a coordinated $NHMe_2$ molecule, which is confirmed by the longer Mo(1)–N(5) bond distance of 2.216(4) Å and the maximum located in the electron-density difference map for the attached proton. The geometry around the five-coordinate molybdenum center is square pyramidal. The metal-nitride bond length of 1.644(3) Å is in accordance with reported values. The phosphorus adopts an inverted stereochemistry relative to **2a** and **2b**, so that the phosphine would need to invert to coordinate

the remaining arm. Although four-coordinate triamido molybdenum nitrides are more typical, related complexes with five-coordinate nitrogen donor environments and unbound ligand arms are known, albeit due to additional chelating amine donors, rather than bound NMe_2H.[16] Although the lone pair of the phosphine is not directed towards the molybdenum centre, the Mo(1)···P(1) separation of 2.974(1) Å is still as short as some of the longer bonding Mo-P interactions reported in the literature.[15]

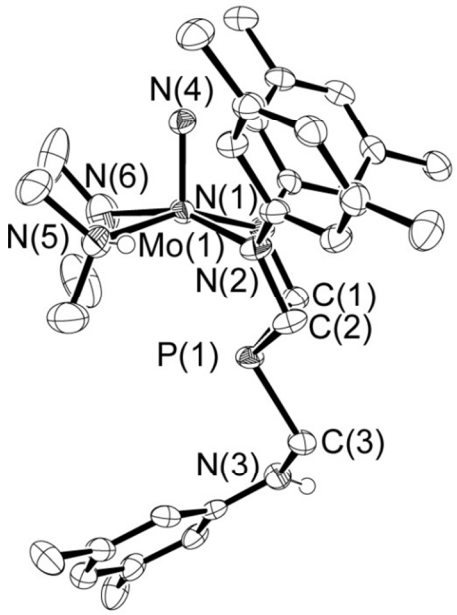

Figure 2. Solid-state molecular structure of **3** as determined by X-ray crystallography. The co-crystallized toluene, fluorine and hydrogen atoms, excluding those attached to N(3) and N(5), have been omitted for clarity. Selected bond lengths or distances (Å): Mo(1)–N(4), 1.644(3); Mo(1)–N(1), 2.080(3); Mo(1)–N(5), 2.216(4); Mo(1)–N(6), 2.009(4). Selected angles in degrees:

N(4)–Mo(1)–N(1), 103.89(14); N(4)–Mo(1)–N(2), 101.77(13); N(4)–Mo(1)–N(5), 98.57(15); N(4)–Mo(1)–N(6), 96.48(16); N(1)–Mo(1)–N(2), 89.89(12); N(5)–Mo(1)–N(6), 86.27(19); N(1)–Mo(1)–N(6), 95.34(16); N(2)–Mo(1)–N(5), 81.29(15), C(1)–P(1)–C(2), 98.20(18); C(1)–P(1)–C(3), 101.13(17); C(2)–P(1)–C(3), 101.39(17).

Attempts to synthesize the C_3 symmetric compound **2c** in greater yield by refluxing **1c** and $(Me_2N)_3Mo{\equiv}N$ for 2 h, failed to produce an increase in yield, with **3** remaining the major product. Since complex **3** has poor solubility in toluene at room temperature, **2c** was isolated by washing the precipitate from the reaction of **1c** and $(Me_2N)_3Mo{\equiv}N$ with liberal amounts of toluene to remove **2c**. Complex **2c** crystallized by slow evaporation of a toluene solution at −40 °C but provided only small orange plates that diffracted X-rays poorly, and thus only served to confirm connectivity. Details are provided in the Supporting Information.

Compounds **2a-c** are slightly solubility in the aromatic solvents benzene and toluene, and are very soluble in CH_2Cl_2. The ^{1}H NMR spectra for complexes **2a**, **2b**, and **2c** are consistent with C_{3v}-symmetric species with only one ligand environment. These symmetric species display $^{31}P\{^1H\}$ NMR resonances at δ –55.7, –56.3 and –55.4, respectively. These resonances are significantly shifted upfield from that of the ligand precursors, which have $^{31}P\{^1H\}$ NMR shifts of δ −29.6, −31.0, −32.6 respectively.[3a] The Tolman cone angles of **2a-c** are 99.3, 97.8 and 98.3 °, respectively, which is significantly smaller than the value of 118 ° for PMe_3. Percent buried volumes provides an alternate evaluation of steric properties; for **2a-c** the percent buried volumes were calculated[17] to be 23.1, 23.2 and 23.2 %, respectively, which is similar to the value of 22.2 % reported for PMe_3.[18]

Complex **3**, which when isolated has only trace solubility in toluene or benzene at room temperature, is soluble in THF, CH_2Cl_2 and chloroform, but slowly decomposes under these conditions. Complex **3** has a $^{31}P\{^1H\}$ NMR resonance at δ –52.8, a shift that is similar to **2a-c**. The 298 K ^1H NMR spectrum of **3** in THF-d_8 confirms the presence of the co-crystallized toluene, and displays some broad resonances due to fluxionality. Variable-temperature ^1H and ^{19}F NMR spectroscopy are consistent with a fluxional process where the bound NMe_2H dissociates and renders the two bound ligand arms chemically equivalent, while maintaining the uncoordinated ligand arm unique, as shown in Scheme 2. Cooling to 273 K provided a spectrum consistent with the symmetry of the complex in the solid state. A pair of sharp singlets for the Mo–NMe_2 moiety are observed at δ 3.64 and 4.80, suggestive of a significant barrier to rotation about the Mo–N amido bond, and these resonances do not broaden upon warming, thus ruling out a fluctional process where a proton is transferred from the coordinated amine to the amido moiety. Two diastereotopic resonances at δ 2.38 and 2.87 are observed for the methyl groups associated with the coordinated NMe_2H moiety at 273 K, both of which are doublets from coupling to the NH proton, with a $^3J_{HH}$ of 5 Hz. These broaden and coalesce at 313 K. A dissociative exchange process is suggested by the fact that the widths of the two peaks prior to coalescence is not the same, with a significantly broader peak for the resonance at δ 2.87 compared to the resonance at δ 2.38, suggestive of exchange with free NMe_2H in solution. Unbound NMe_2H could not be assigned in any of the variable-temperature ^1H NMR spectra, although it is likely that dissociation of NMe_2H in THF provides the intermediate to chemical exchange $P(CH_2N\text{-}3,5\text{-}(CF_3)_2C_6H_3)_2(CH_2NH\text{-}3,5\text{-}(CF_3)_2C_6H_3)(Me_2N)Mo{\equiv}N$. Such a dissociative equilibrium should be increasingly thermodynamically disfavoured at lower temperatures, which would explain the absence of unbound NMe_2H at the slow-exchange limit. The resonances

associated with the bound ligand arms also undergo exchange, consistent with the proposed mechanism of exchange, with two broad *ortho*-H environments at 273 K, which coalesce at 303 K to provide a single environment. The four overlapped CH_2 environments observed at 273 K also coalesce into a doublet and a doublet of doublets above 298 K. The multiplet patterns are suggestive of an AB coupling between these diastereotopic CH_2 environments, consistent with the mirror plane of symmetry in the proposed intermediate to exchange. Although it is anticipated that there should two diastereotopic ^1H environments for the PCH_2 moiety of the unbound ligand, these must be nearly coincident, because a single PCH_2 environment is observed at all temperatures. The line-shapes in the variable-temperature ^1H and ^{19}F NMR spectra spectra were modeled using the WinDNMR[19] simulation program and the Arrhenius equation to estimate an activation energy of 5 kcal·mol^{-1} for this exchange process.

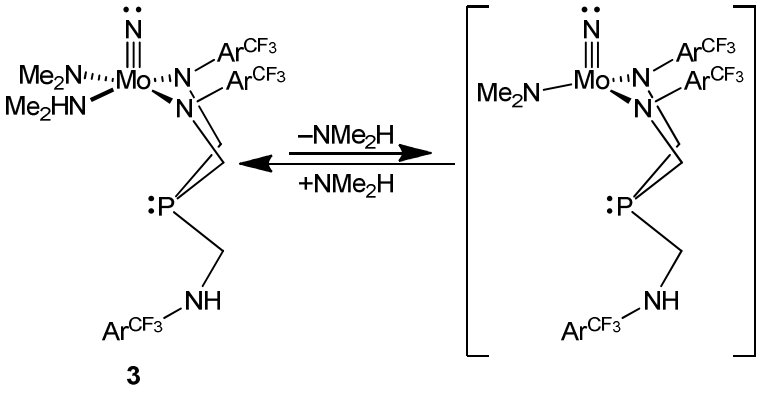

Scheme 2. Proposed mechanism for fluctionality in **3** in THF.

The equilibrium dissociation of coordinated NMe_2H from **3** suggests that conversion to **2c** should be facile in THF above room temperature; however, this proved not be true. Heating solutions of **3** in THF led to decomposition, with increasing amounts of **1c** observed by $^{31}P\{^1H\}$

NMR. Attempts were also made to increase the yield of compound **2c** obtained in the reaction of **1c** and $(Me_2N)_3Mo{\equiv}N$ and Lewis acids to trap the NMe_2H . Employing $B(C_6F_5)_3$ as a Lewis acid to abstract the coordinated dimethylamine resulted in an slight initial increase in the amount of **2c**, but also several other byproducts, and ultimately decomposition. The difficulty in forming **2c** may due to the poorer electron-donating capabilities of this ligand, which when combined with the strained angles enforced by the chelate, outweighs the typical thermodynamic advantage of the claw-like coordination mode. Due to the poor yield of **2c**, it was not used in further synthetic studies.

Tungsten complexes similar to compounds **2a-c** are capable of participating in catalytic nitrile-alkyne cross metathesis,[10a, b] and Mo complexes that perform these reactions have also been studied.[10c] Given the novel unusual bond-angles imparted by the ligands in **2a-c** and **3**, we attempted alkyne-nitrile cross-metathesis reactions. Unfortunately, attempted reactions with $MeC{\equiv}^{15}N$,[20] diphenylacetylene and 3-hexyne at elevated temperatures in toluene or THF all failed to provide metathesis products.

Dinuclear Mo-V complexes. The reaction of **2a** with $V(Mes)_3THF$ (Mes = 2,4,6-$Me_3C_6H_2$) in toluene for 3 days at room temperature afforded the brown nitrido-bridged complex, $P(CH_2NAr^R)_3Mo(\mu\text{-}N)V(Mes)_3$ (**4a**), as shown in eq 3. A similar reaction between **2b** and $V(Mes)_3THF$ also provided a brown solid that is presumed to be the analogue **4b**, but repeated attempts at crystallization of this solid failed.

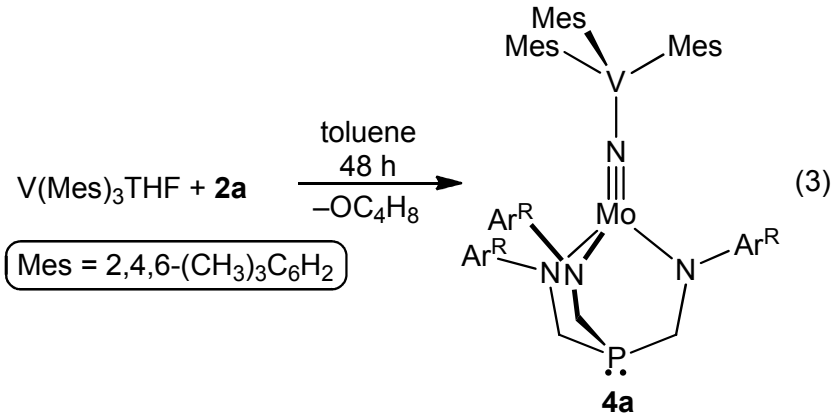

(3)

X-ray quality crystals were obtained by slow evaporation of toluene solution of **4a** at room temperature, and an ORTEP of the solid-state molecular structure is shown in Figure 3. The complex has no crystallographic symmetric, but has approximate C_3 symmetry. There are two molecules in the asymmetric unit with three co-crystallized toluene molecules, one of which is disordered.

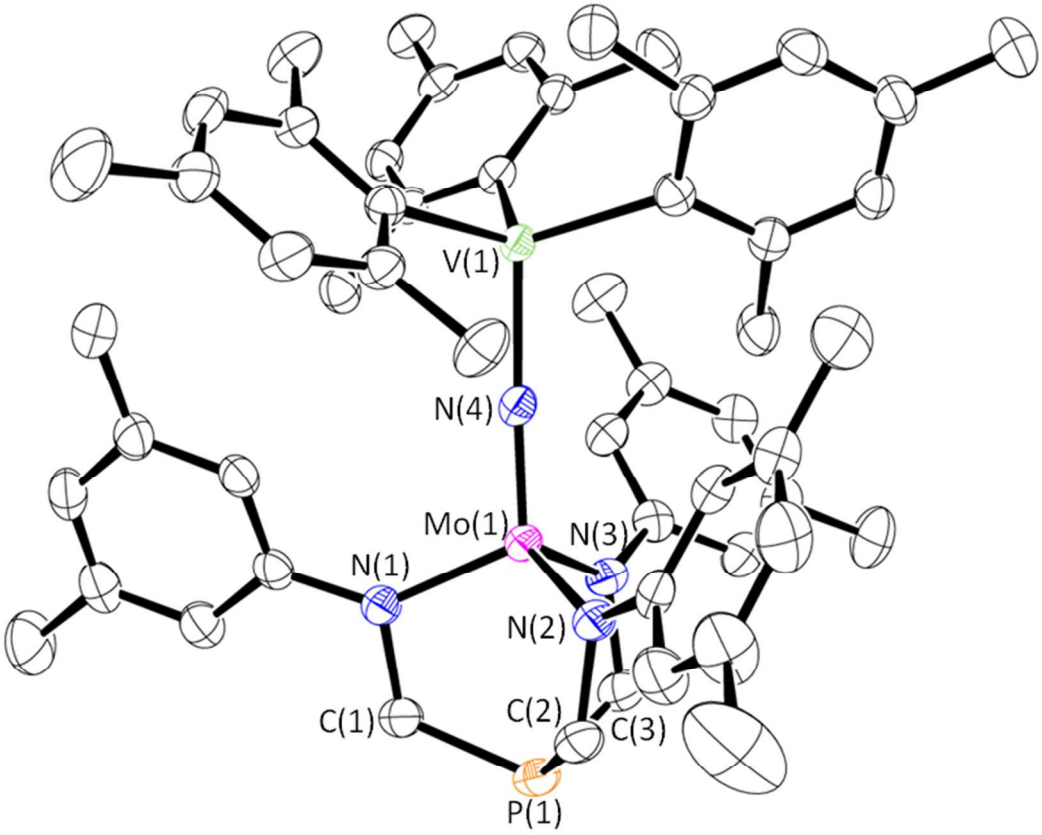

Figure 3. Solid-state molecular structure of **4a** as determined by X-ray crystallography. The hydrogen atoms and co-crystallized toluene have been removed for clarity. Selected bond lengths (Å): Mo(1)–N(4), 1.694(2); Mo(1)–N(1), 1.954(2); V(1)–N(4), 2.019(2); Mo(1)···P(1), 2.9541(8). Selected angles in degrees: Mo(1)–N(4)–V(1), 176.70(13); N(4)–Mo(1)–N(1), 112.19(10); N(1)–Mo(1)–N(2), 108.25(9).

The approximately tetrahedral geometry around Mo in **4a** is similar to **2a**. The Mo–N(4)–V(1) angle of 176.70(13)° is approximately linear. The Mo(1)–N(4) bond length of 1.694(2) Å is 0.044(3) Å longer than in **2a**. This distance is significantly less than for Mo=N double bonds in similar coordination modes,[9b, 21] and similar to the Mo≡N distance of 1.678(4) for the related

complex of a neutral lone pair acceptor $(3,5\text{-}Me_2C_6H_3N^tBu)_3Mo{\equiv}NBF_3$.[13] The V–N(4) bond length of 2.019(2) Å, consistent with a single bond, but similar bridging-nitrido complexes of V(III) and V(IV) are not available for comparison. The V–N(4) distance is long compared to V(IV) amido complexes such as $V(NMe_2)_4$,[22] but comparable to V(III) complexes such as $V(NPh_2)_4Li(THF)_4$,[23] though the differences between bridging nitride and amido metal-nitrogen distances renders a decisive assignment of oxidation states based on this distance impossible. The V–C bond distances in **4a** range from 2.090(3) to 2.125(3), similar to both V(III) and V(IV) complexes, but longer than V(V) complexes such as $Mes_3V{=}O$ or $Mes3V{=}N{-}GePh_3$.[24] It is somewhat ambiguous from this data if the complex is best regarded as a Mo(VI)–V(III) complex or a Mo(V)-V(IV) complex. A related complex, $[N_3N]WCOVMes_3$, obtained from the reaction of Mes_3V and $[N_3N]W(CO)$, where $[N_3N] = N(CH_2CH_2NC_6F_5)_3$, was found to form via a one-electron oxidation of V to V(IV), but this provides a formally W(VI) centre, and formal reduction of the CO ligand.[25] Density functional theory calculations on **4b** predict that it should be a ground state triplet with SOMOs that are vanadium- and molybdenum-based non-bonding π-interactions across the nitride donor, but the unrestricted B3LYP method used is most likely not sophisticated enough to accurately predict the ground state.

To gain insight into the electronic structure of these complexes the magnetic susceptibilities of complex **4a** were obtained in both the solution and solid state. A room-temperature toluene solution of **4a** was determined by Evans's method to have χ_mT values of 1.01 $cm^3{\cdot}K{\cdot}mol^{-1}$. Room-temperature Gouy measurements of a powdered sample of **4a** was determined to have comparable χ_mT values of 1.30 $cm^3{\cdot}K{\cdot}mol^{-1}$, calibrated to an external $Hg[Co(SCN)_4]$ standard. All values are corrected for diamagnetic contributions, estimated using Pascal's constants. Both solution and solid-state results confirm the presence of two unpaired

electrons, and are suggestive of an $S = 1$ ground state. This is consistent with either a Mo(VI)–V(III) or Mo(V)–V(IV) formulation of the complex, providing the latter still features strong coupling between the electrons. Variable-temperature magnetic susceptibility data collected on a SQUID magnetometer revealed a gradual decline in $\chi_m T$ for **4a** below 50 K, consistent with a small zero-field splitting of a triplet ground state with $D = 2.5$ cm^{-1}. The EPR spectra of solid samples of **4a** cooled in liquid nitrogen provided only uninformative broad peaks, the most prominent of which appeared to be a $g_\perp$ signal at 1.934. Although the $g_\parallel$ peak appeared to exhibit hyperfine coupling to other nuclei, such as V ($I = 7/2$), and were centred closer to $g = 2$, the broad line widths prevented any modeling, assignment or interpretation.

Multiple attempts under a variety of conditions were made to react **4a** with **1b**, to generate complexes of the type $P(CH_2NAr^R)_3Mo(\mu\text{-}N)V(PhNCH_2)_3P$, but all reactions failed to produce any isolable complex. The precursor $Mes_3V(THF)$ also failed to react cleanly with **1a-c**, which could provide an alternate route to a linear diphosphine.

Nickel Complexes. As noted in the introduction, we found that through-space exchange coupling was possible between metal centres coordinated to the amido donors and phosphine donors in binuclear complexes supported by the $P(CH_2NAr^R)_3$ ligands. For example, through-space exchange coupling was observed between Gd(III) and Co(II) was possible in the complex [TPP]CoP($CH_2NC_6H_4$-2-CO_2Me_3Gd (where [TPP] = 5, 10, 15, 20-tetrakis(4-methoxyphenyl)porphine).[3b] This coupling relies on the unpaired electron on Co(II) being associated with an antibonding interaction with the phosphine lone pair, which accumulates spin density near the Gd(III) centre. Unfortunately, it has not been possible to bind two phosphine donors to Co[TPP], to generate trinuclear complexes or polymers with exchange-coupling mediated by a through-space mechanism. We attempted to use $Ni(acac)_2$ (where acac =

acetylacetonate) as an alternate centre to generate extended complexes of this type. This d^8 octahedral metal centre should also have antibonding interactions between the phosphine donor and nickel based unpaired electrons in the d_z^2 orbital. The reaction of two equivalents of **2a** with $Ni(acac)_2$ in THF was intended to produce *trans*-$Ni(acac)_2[P(CH_2N\text{-}3,5\text{-}(CH_3)_2C_6H_3)_3)_3Mo{\equiv}N]_2$; related phosphine complexes of $Ni(acac)_2$ are known.[26] Instead, this reaction produced the Ni(0) complex $Ni[P(CH_2N\text{-}3,5\text{-}(CH_3)_2C_6H_3)_3)_3Mo{\equiv}N]_4$ (**5a**), albeit in very poor yield, as confirmed by NMR spectroscopy and single crystal X-ray diffraction An improved route to this complex is from the reaction of four equivalents of **2a** with $Ni(COD)_2$ (where COD =1,5-cyclooctadiene). Similarly, the reaction four equivalents of **2b** with $Ni(COD)_2$ provided $Ni[P(CH_2NPh)_3Mo{\equiv}N]_4$ (**5b**). Complex **5b** was also a product of the reaction of $Ni(acac)_2$ with **2b**, as confirmed by $^{31}P\{^1H\}$ NMR spectroscopy, although this is not a high-yielding route. The reduction of the $Ni(acac)_2$ precursor in its reaction with **2a** appears to occur due to the reactivity of the metal-amido bonds.

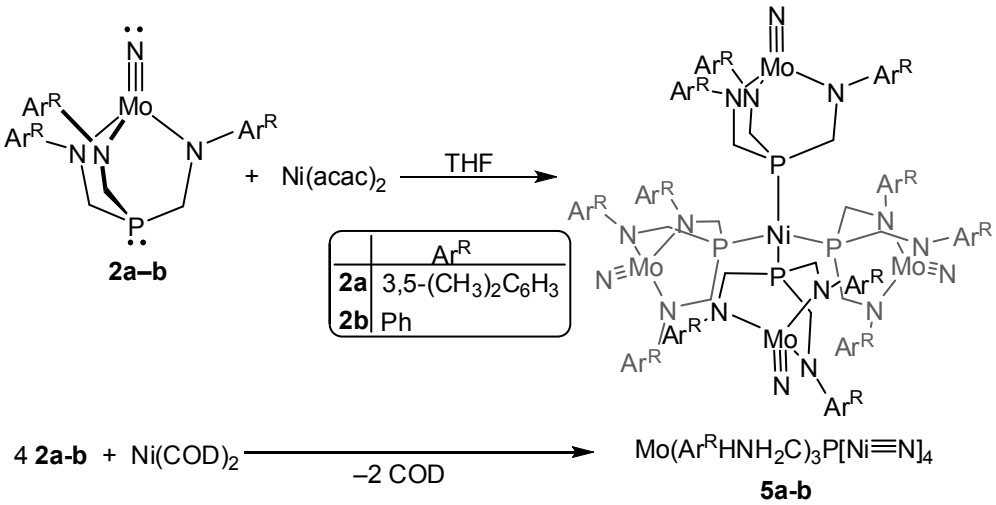

Scheme 3.

The orange crystalline precipitate of **5b** obtained from either synthetic route were suitable for X-ray crystallography, and its ORTEP solid-state molecular structure is shown in Figure 4. There are two molecules in the asymmetric unit, and both lie on a crystallographic C_3 axis. There are two co-crystallized THF molecules that are partially removed *in vacuo*. X-ray quality crystals precipitated from the crude reaction mixture of **5a** as well; however, the solid-state structure of **5a** the molecule suffers from extensive disorder of ten cocrystallized THF molecules in the unit cell. Although the connectivity of **5a** was confirmed, a high quality solution could not be obtained, though there is no reason to believe the structure to be significantly different from **5b**.

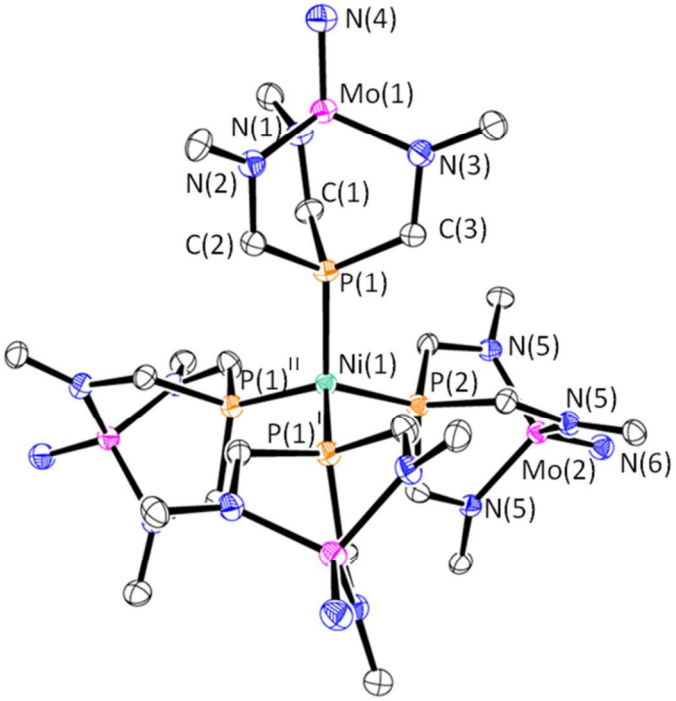

Figure 4. ORTEP of the solid-state molecular structure of **5b** as determined by X-ray crystallography. The second molecule in the asymmetric unit, co-crystallized THF molecules, phenyl rings, except *ipso* carbons, and hydrogen atoms have been removed for clarity. Selected

bond lengths (Å): Ni(1)–P(1), 2.1615(9); Ni(1)–P(2), 2.1583(16); Mo(1)–N(4), 1.662(3); Mo(1)–N(2), 1.951(3). Selected angles in degrees: P(1)–Ni(1)–P(2), 109.48(3); N(1)–Mo(1)–N(4), 111.24(13); N(1)–Mo(1)–N(2), 106.75(12).

The nickel center has four phosphines coordinated in a tetrahedral arrangement with an average Ni–P bond length of 2.16 Å which is comparable to similar nickel complexes reported in literature.[27] The $P(CH_2NPh)_3Mo{\equiv}N$ subunits in **5b** show no significant differences in comparison to **2b**. Complexes **5a-b** have only trace solubility in THF, are soluble in toluene and chloroform, but decompose over time. Analyses of the crude reaction mixtures by ^1H and $^{31}P\{^1H\}$ NMR spectroscopy revealed no significant side products were formed. The complexes display $^{31}P\{^1H\}$ NMR resonances at δ −1.2 and −1.3 for **5a** and **5b**. Related complexes with moderately sized phosphines such as $Ni(PEt_3)_4$ are known to dissociate a phosphine donor in solution, however, the $^{31}P\{^1H\}$ NMR spectra give no indication of phosphine dissociation from **5a-b** in solution, consistent with the phosphine donors **2a-b** having very small cone-angles. Similar nickel tetraphosphine complexes are also known to undergo one-electron oxidation at the Ni centre to provide paramagnetic Ni(I) complexes. However, attempts to oxidize the Ni centres in these pentanuclear clusters using AgCN or $AgBF_4$ produced a black precipitate, but no new species by ^1H NMR or EPR spectroscopy.

Reaction of either **5a** with $V(Mes)_3THF$ or **4a** with $Ni(COD)_2$ are both viable routes to the paramagnetic nonanuclear complexes $Ni[P(CH_2NAr^R)_3Mo(\mu\text{-}N)VMes_3]_4$ (**6a**), as shown in Scheme 4. In the case of the reaction of **5a** with $V(Mes)_3THF$ in THF, the reaction was slow due to the modest solubility of **5a** in THF, and the reaction provided large (~4 mm^3) brown crystals of the product. Attempts to form the analogue **6b** provided a brown powder, but X-ray quality crystals could not be obtained to ascertain structure. Despite the crystals of **6a** having well-

defined edges and smooth faces, they diffracted poorly. The unit cell was determined to be tetragonal, though the diffraction pattern was suggestive of twinning. No space group selection gave a high quality structure, although disordered solutions that demonstrated connectivity could be obtained in both $I\bar{4}$ and $P\bar{4}2_1c$ The nickel atom resides at the −4 symmetric position. Locating the P, Mo, V and bridging-nitride N atoms that lie in an approximately linear arrangement in the electron-density difference map and refining their positions proved straightforward, but extensive disorder of the remaining ligands and multiple disordered co-crystallized THF molecules prevented an adequate structure solution from being obtained; an ORTEP depiction is shown in Scheme 4 only to demonstrate connectivity. The model is deficient, with multiple restraints used in the solution, no attempt to model disordered THF molecules in the large void spaces, and isotropic treatment of all atoms. It is unclear if the poor quality structure is due to extensive disorder of the orientation of the supporting $P(CH_2NAr^R)_3$ and Mes ligands, twinning, or a combination of these factors. Attempts to model the reflection data in lower symmetry space groups did not provide a better model.

The Ni centre in **6a** is Ni(0), with a d^{10} electronic configuration, and variable-temperature magnetic susceptibility data collected on a SQUID magnetometer investigated to determine if the accumulation of unpaired spin-density on the phosphorus donor was sufficient to allow coupling between $P(CH_2NAr^{Me})_3Mo(\mu\text{-}N)VMes_3$ units via polarization of the spin on the Ni centre. The observed data is consistent with only minimal interaction between the triplet state $P(CH_2NAr^{Me})_3Mo(\mu\text{-}N)VMes_3$ units. Similar to the data for **4a**, χ_mT declines only slightly after 50 K. Although this could be due to coupling, a better fit was obtained by assuming that the drop in χ_mT and low temperatures was due to zero-field splitting, and the data can be fit with a

triplet ground state of the $P(CH_2NAr^{Me})_3Mo(\mu\text{-}N)VMes_3$ units with $D = 3.2\ cm^{-1}$, after correction for a modest temperature-independent paramagnetism, possibly due to trace Ni metal.

Scheme 4.

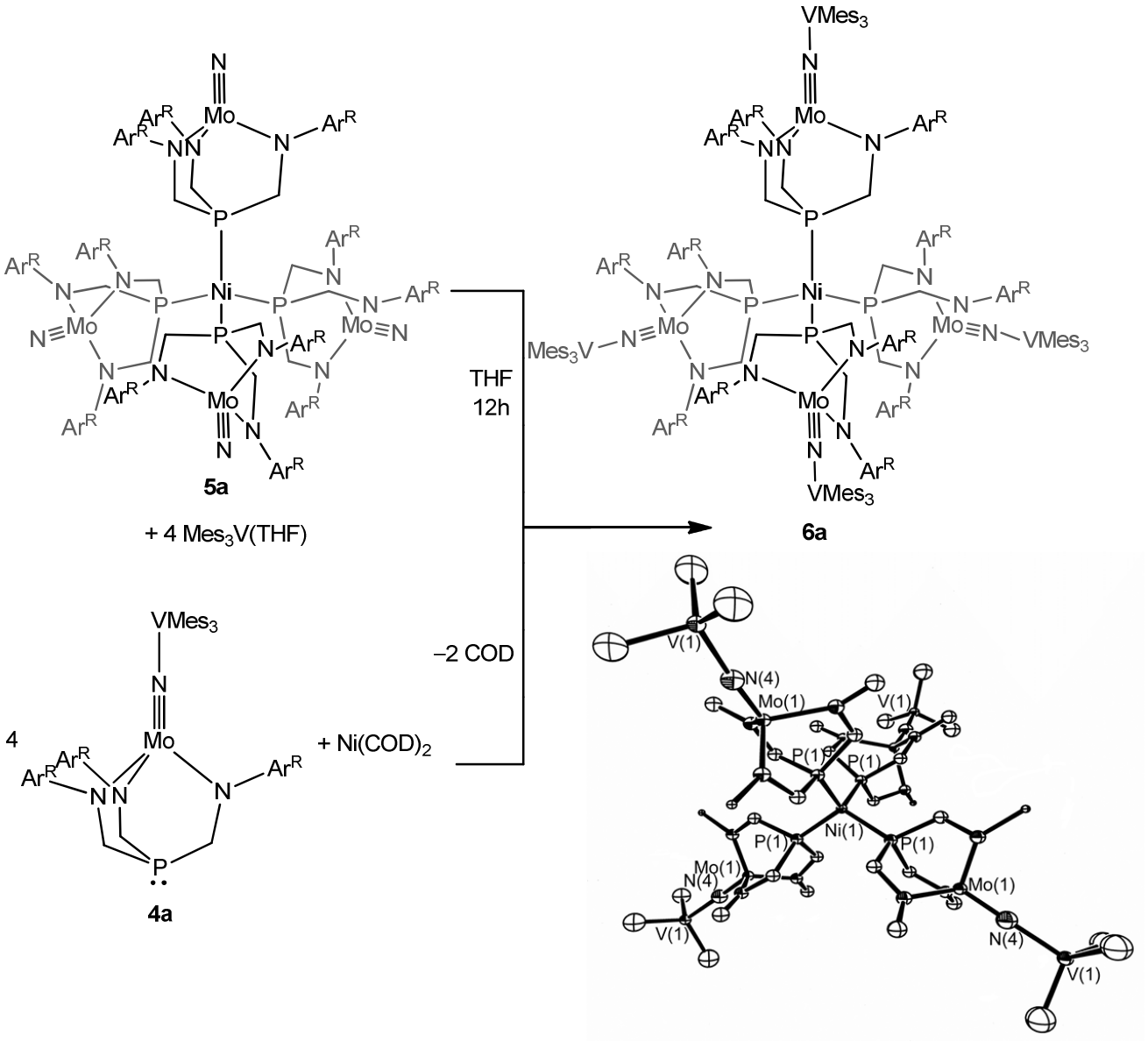

Conclusions

The complexes $P(CH_2NAr^R)_3Mo{\equiv}N$ with Ar^R = 3,5-$(CH_3)_2C_6H_3$ (**2a**) or Ph (**2b**) or were both readily obtained by the reaction of $P(CH_2NHAr^R)_3$ with $(Me_2N)_3Mo{\equiv}N$, whereas the use of the more electron-withdrawing substituent Ar^R = 3,5-$(CF_3)_2C_6H_3$ provided only small amounts of the desired complex **2c**, with $P(CH_2N\text{-}3,5\text{-}(CF_3)_2C_6H_3)_2(CH_2NH\text{-}3,5\text{-}(CF_3)_2C_6H_3)(NMe_2H)(NMe_2)Mo{\equiv}N$ (**3**) as the major product. Unfortunately, these complexes failed to show any π-bond metathesis reactions with $MeC{\equiv}^{15}N$,[20] diphenylacetylene and 3-hexyne at elevated temperatures. However, they did behave as ditopic ligands, binding to the $V(Mes)_3$ moiety via the molybdenum-nitrido, and to Ni(0) via the phosphine,, which allowed for the formation of the dinuclear complexes $P(CH_2NAr^R)_3Mo(\mu\text{-}N)V(Mes)_3$ (**4a-b**), pentanuclear complexes $Ni[P(CH_2NAr^R)_3Mo{\equiv}N]_4$ (**5a-b**) and the nonanuclear complex $Ni[P(CH_2NAr^R)_3Mo(\mu\text{-}N)VMes_3]_4$ (**6a-b**). Although these compounds were of interest as possible phosphine donors that could also shuttle electrons to a catalytic site, all attempts to conduct cyclic voltammetry experiments failed to reveal reversible redox couples. Less reactive metal centres than V(III) are currently under investigation as an alternative.

Experimental Section

General Procedures. Unless otherwise stated, all manipulations were performed under an inert atmosphere of nitrogen using either standard Schlenk techniques or an MBraun glovebox. Dry, oxygen-free solvents were employed throughout. Anhydrous pentane, toluene, diethyl ether, THF, CH_3CN, and CH_2Cl_2 were purchased from Aldrich, sparged with dinitrogen, and passed through activated alumina under a positive pressure of nitrogen gas; toluene and hexanes were further deoxygenated using Ridox catalyst columns.[28] Deuterated benzene was dried by heating

at reflux with sodium/potassium alloy in a sealed vessel under partial pressure then trap-to-trap distilled and freeze-pump-thaw degassed three times. Deuterated toluene was purified in an analogous manner by heating at reflux over Na. Deuterated THF was purified in an analogous manner by heating at reflux over K. Deuterated chloroform was dried by heating over activated alumina. NMR spectra were recorded on a Bruker AMX 300 MHz or 500 MHz spectrometer. All chemical shifts are recorded in parts per million, and all coupling constants are in hertz. ^{1}H NMR spectra were referenced to residual protons (C_6D_5H, δ 7.16; C_7D_7H, δ 2.09; $CDHCl_2$, δ 5.32; C_4D_7HO, δ 1.73; $CHCl_3$, δ 7.26) with respect to tetramethylsilane at δ 0.00. $^{31}P\{^{1}H\}$ NMR spectra were referenced to external 85% H_3PO_4 at δ 0.00. For $^{19}F\{^{1}H\}$ NMR spectra, CCl_3F was used as the external reference at δ 0.00. $^{13}C\{^{1}H\}$ NMR spectra were referenced to solvent resonances (C_6D_6, δ 128.0; C_7D_8, δ 20.4; CD_2Cl_2, δ 53.8; C_4D_8O, δ 67.4; $CDCl_3$, δ 77.0). EPR spectra were collected using an X-band Bruker ESR 300E spectrometer. Unless otherwise noted, variable-temperature magnetic susceptilibilty measurements were performed at 10 000 Oe with a Quantum Design Evercool MPMS-XL7 system. Corrections for the diamagnetic contributions of compounds were made using Pascal's constants. Samples were run in a PVC holder specially designed to possess a constant cross-sectional area. Alternate determination of magnetic susceptibility was carried out using a Johnson Matthey Magnetic Susceptibility Balance, MSB I, referenced to an external standard, $Hg[Co(SCN)_4]$. Cyclic voltammetry was performed using a Bioanalytical Systems 100B/W electrochemical analyzer. Elemental analyses were either performed by Atlantic Microlab Inc, Atlanta, Georgia, USA, or the Centre for Catalysis and Materials Research, Windsor, Ontario, Canada. Complexes 4a, 5a-b and 6a repeatedly gave low C values despite being uniform crystalline solids with acceptable H and N analyses. The ligand

precursors (**1a-c**),[3a] VMes(THF),[29] $(Me_2N)_3Mo{\equiv}N$,[9b] and nickel bis(1,5-cyclooctadiene)[30] were prepared by literature methods.

Synthesis of $P(CH_2N\text{-}3,5\text{-}(CH_3)_2C_6H_3)_3Mo{\equiv}N$ (2a). A toluene solution (10 mL) of $P(CH_2NH\text{-}3,5\text{-}(CH_3)_2C_6H_3)_3$ (**1a**) (800 mg, 2.13 mmol) and $N{\equiv}Mo(NMe_2)_3$ (516 mg, 2.13 mmol) was stirred for 15 min then left undisturbed on the shelf overnight at room temperature. Red-orange X-ray quality crystals precipitated from solution. The solid was filtered, washed with 10 mL of cold pentane, and dried under vacuum (764 mg, 66 % yield). The filtrate was dried in vacuo to give a black solid that was washed with 5 mL of pentane and dried. Recrystallization from toluene at room temperature yielded a brown-orange solid (130 mg, 11 % yield) that was confirmed to be a second crop of the desired product by NMR (77 % total yield). ^{1}H NMR (toluene-d_8, 25 °C, 500.13 MHz): δ 2.2 (s, 18H, CH_3); 3.8 (d, 6H, CH_2, $^2J_{PH}$ = 8.4 Hz); 6.58 (s, 3H, *p*–H); 7.42 (s, 6H, *o*–H). ^{31}P{^{1}H} NMR (toluene-d_8, 25 °C, 202.5 MHz): δ –55.7 (s). ^{13}C{^{1}H} NMR (toluene-d_8, 25 °C, 125.8 MHz): δ 21.6 (s, *C*H_3); 45.4 (d, P*C*H_2, $^1J_{PC}$ = 28 Hz); 115.0 (s, *p*–C); 125.0 (s, *m*–C); 138.3 (s, *o*–C); 150.8 (s, *ipso*-C). Anal. Calcd for $C_{27}H_{33}MoN_4P$ (f.w. 540.5 g mol^{-1}): C, 60.00; H, 6.15; N, 10.37. Found: C, 59.74; H, 6.18; N, 10.15.

Synthesis of $P(CH_2NPh)_3Mo{\equiv}N$ (2b). A toluene solution (15 mL) of $P(CH_2NHC_6H_5)_3$ (**1b**) (1.44 g, 4.13 mmol) and $N{\equiv}Mo(NMe_2)_3$ (1 g, 4.13 mmol) was stirred for 15 min then left undisturbed for 8 h. Orange X-ray quality crystals precipitated from solution. The orange solid was filtered, washed with 10 mL of cold pentane, and dried under vacuum (1.39 g, 74 % yield). The filtrate was dried in vacuo to give a black solid that was washed with 10 mL of pentane. Recrystallization from toluene at room temperature yielded a second crop of the product as a brown-red solid (280 mg, 15 % yield) that was confirmed to be the desired product by NMR (89 % total yield). ^{1}H NMR (toluene-d_8, 25 °C, 500.13 MHz): δ 3.53 (d, 6H, CH_2, $^2J_{PH}$ = 8.4 Hz);

6.88 (d, 6H, *o*–H, $^{3}J_{HH}$ = 8 Hz); 7.16 (dd, 6H, *m*–H, $^{3}J_{HH}$ = 8 Hz); 7.66 (t, 3H, *p*–H, $^{3}J_{HH}$ = 8 Hz). $^{31}P\{^{1}H\}$ NMR (toluene-d_8, 25 °C, 202.5 MHz): δ –56.3 (s). $^{13}C\{^{1}H\}$ NMR (toluene-d_8, 25 °C, 125.77 MHz): δ 45.3 (d, P*C*H$_2$, $^{1}J_{PC}$ = 30 Hz); 117.0 (s, *p*–C); 123.2 (s, *m*–C); 128.5 (s, *o*–C); 150.5 (s, *ipso*–C). Anal. Calcd for $C_{21}H_{21}MoN_4P$ (f.w. 456.3 g mol^{-1}): C, 55.27; H, 4.64; N, 12.28. Found: C, 55.59; H, 4.70; N, 11.94.

Synthesis of P(CH$_2$N-3,5-(CF$_3$)$_2$C$_6$H$_3$)$_3$Mo≡N (2c) and P(CH$_2$N-3,5-(CF$_3$)$_2$C$_6$H$_3$)$_2$(CH$_2$NH-3,5-(CF$_3$)$_2$C$_6$H$_3$)(NMe$_2$H)(NMe$_2$)Mo≡N ·C$_7$H$_8$ (3). A toluene solution (25 mL) of P(CH$_2$NH-3,5-(CF$_3$)$_2$C$_6$H$_3$)$_3$ (**1c**) (3.13 g, 4.13 mmol) and N≡Mo(NMe$_2$)$_3$ (1 g, 4.13 mmol) was stirred for 15 min then left undisturbed for 14 h. Red X-ray quality crystals of **3** precipitated from solution containing a co-crystallized toluene molecule, which could not be removed in vacuo, along with the brown powder N≡MoP(CH$_2$N-3,5-(CF$_3$)$_2$C$_6$H$_3$)$_3$ (2c) in a 5:1 ratio, respectively. The mixture was filtered, washed with 50 mL of cold pentane to remove trace **1c**, and dried under vacuum (3.18 g). Compound **3** has only trace solubility in toluene at room temperature. A relatively pure sample of **2c** could be obtained by stirring the solid obtained in 25 mL of toluene at room temperature overnight. The red solid (**3**) was filtered off, rinsed with 10 mL of toluene, then 15 mL of pentane, and dried under vacuum to provide 2.51 g of solid, albeit with some remaining **2c** by ^{1}H and $^{31}P\{^{1}H\}$ NMR spectroscopy. The filtrate was evaporated to dryness yielding a brown-orange solid (**2c**), further washed with 15 mL of pentane, and dried under vacuum (350 mg, 9.8 % yield). Crystalline plates were obtained from toluene, but X-ray crystallography allowed only for the confirmation of connectivity.

For **2c**: ^{1}H NMR (THF-d_8, 25 °C, 300.13 MHz): δ 4.55 (d, 6H, C*H*$_2$, $^{2}J_{PH}$ = 7.5 Hz); 7.57 (s, 3H, *p*–H); 8.16 (s, 6H, *o*–H). $^{31}P\{^{1}H\}$ NMR (THF-d_8, 25 °C, 121.5 MHz): δ −55.4 (s). $^{13}C\{^{1}H\}$ NMR (THF-d_8, 25 °C, 75.5 MHz): δ 47.3 (d, P*C*H$_2$, $^{1}J_{PC}$ = 30 Hz); 116.0 (br m, Ar-*C*F$_3$); 117.3, 122.9

and 126.4 (s, *o*–, *m*– and *p*–C); 152.7 (s, *ipso*–C). $^{19}F\{^{1}H\}$ NMR (THF-d_8, 25 °C, 282.5 MHz): δ −65.9 (s). Anal. Calcd for $C_{27}H_{15}F_{18}MoN_4P$ (f.w. 864.34): C, 37.52; H, 1.75; N, 6.48. Found: C, 37.67; H, 1.86; N, 6.31.

For **3**: ^{1}H NMR (THF-d_8, 25 °C, 300.13 MHz): δ 2.38 and 2.87 (d, 3H each, HN*Me*$_2$, $^{3}J_{HH}$ = 5.8 Hz); 3.63 and 4.71 (s, 3H each, MoN*Me*$_2$); 3.79 and 3.88 (ABX, 2H each, bound arm PC*H*$_2$); coincident at 4.18 (ABX, 2H, unbound arm PC*H*$_2$); 6.55 (dd, 1H, N*H*, $^{3}J_{HH}$ = 5.8, 5.8 Hz); 7.10 (overlapped s, 3H, free arm *o*-H and *p*-H) 7.22 (s, 2H, bound arm *p*-H), 7.65 and 7.99 (br, 2H each, bound arm *o*-H). $^{31}P\{^{1}H\}$ NMR (THF-d_8, 25 °C, 202.5 MHz): δ –52.8. $^{19}F\{^{1}H\}$ NMR (THF-d_8, 25 °C, 282.5 MHz): δ –65.5 (br, 12F); –65.7 (s, 6F). After drying under high vacuum for 12 h, the sample analyzed consistent with the formulation P(CH_2N-3,5-$(CF_3)_2C_6H_3)_2$(CH_2NH-3,5-$(CF_3)_2C_6H_3$)(NMe_2)Mo≡N·C_7H_8 Anal. Calcd for $C_{36}H_{30}F_{18}MoN_5P$: C, 43.17; H, 3.02; N, 6.99. Found: C, 42.91; H, 3.40; N, 6.93.

Synthesis of P(CH_2N-3,5-$(CH_3)_2C_6H_3)_3$Mo(*μ*-N)V$(Mes)_3$ (4a). A mixture of **2a** (562 mg, 1 mmol) and V$(Mes)_3$THF (500 mg, 1 mmol) was stirred in 20 mL of toluene for 3 days at room temperature, over which time the colour changed from purple to brown. The solvent was removed in vacuo and the brown solid was washed with 10 mL of pentane, and dried under vacuum to provide a paramagnetic solid. Crystals were obtained through slow evaporation of a cold toluene solution, and were found to contain 1.5 equivalents of co-crystallized toluene (910 mg, 92.2 %). The solvent was only partially removed in vacuo. Anal. Calcd for $C_{54}H_{66}MoN_4PV·0.5C_7H_8$: C, 69.40; H, 7.09; N, 5.63. Found: C, 64.73; H, 6.95; N, 5.53. Elemental analyses on multiple samples had appropriate N and H analyses, but suffered from consistently low C values..

Synthesis of Ni[P(CH$_2$N–3,5–(CH$_3$)$_2$C$_6$H$_3$)$_3$Mo≡N]$_4$ (5a). A mixture of **2a** (500 mg, 0.925 mmol, 4 equiv) and Ni(COD)$_2$ (63.6 mg, 0.231 mmol) was dissolved in 5 mL of THF, stirred for 10 min, and left undisturbed on the shelf overnight. Orange coloured X-ray quality crystals precipitated from solution. The crystals were filtered, washed with 10 mL of cold pentane, and dried under vacuum (432 mg, 85 %). Concentration of the mother liquor failed to yield a suitable second crop. ^{1}H NMR (CDCl$_3$, 25 °C, 300.13 MHz): δ 2.1 (s, 72H, Ph–C*H*$_3$); 4.55 (br, 24H, C*H*$_2$); 6.64 (br, 12H, Ph *p*–H); 7.13 (br, 24H, Ph *o*–H). ^{31}P{^{1}H} NMR (CDCl$_3$, 25 °C, 121.5 MHz): δ –1.2 (s). ^{13}C{^{1}H} NMR (CDCl$_3$, 25 °C, 75.49 MHz): δ 21.1 (s, Ph–*C*H$_3$); 55.0 (apparent pentet AXX'$_3$, P*C*H$_2$); 114.3 (s, Ph *m*–C); 125.7 (s, Ph *p*–C); 138.7 (s, Ph *o*–C); 150.0 (s, Ph *ipso*–C). Not all the cocrsytallized THF moieties could be removed by drying overnight under vacuum. Anal. Calcd for C$_{108}$H$_{132}$Mo$_4$N$_{16}$NiP$_4$·(C$_4$H$_8$)$_5$: C, 59.56; H, 6.72; N, 8.68. Found: C, 53.53; H, 6.31 ; N, 8.25. Elemental analyses on multiple samples had appropriate N and H analyses, but suffered from consistently low C values.

Alternate synthesis of 5a. On an NMR scale, a mixture of Ni(acac)$_2$ (5 mg, 0.02 mmol) and **2a** (21 mg, 0.04 mmol, 2 equiv) were dissolved in 1 mL of THF whereupon and immediate colour change to brown was observed. The reaction was monitored by multinuclear NMR spectroscopy. After 30 min, resonances associated with **5a** were observed as the major product.

Synthesis of Ni[P(CH$_2$NC$_6$H$_5$)$_3$Mo≡N]$_4$·2 THF (5b). A mixture of **2b** (500 mg, 1.10 mmol, 4 equiv) and Ni(COD)$_2$ (75.3 mg, 0.274 mmol) was dissolved in 5 mL of THF, stirred for 10 min, and left undisturbed on the shelf overnight. Orange X-ray quality crystals precipitated from

solution, and contained 2 co-crystallized THF molecules, as confirmed by NMR spectroscopy. The crystals were filtered, washed with 10 mL of cold pentane, and dried under vacuum (507.5 mg, 91 %). Concentration of the mother liquor failed to yield a suitable second crop. ^{1}H NMR ($CDCl_3$, 25 °C, 300.13 MHz): δ 1.85 (s, 4H, THF); 3.75 (s, 4H, THF); 4.66 (br, 24H, C*H*$_2$); 7.18 (br, 12H, Ph *p*–H); 7.3 (br, 24H, Ph *m*–H); 7.60 (br, 24H, Ph *o*–H). ^{31}P{^{1}H} NMR ($CDCl_3$, 25 °C, 121.5 MHz): δ –1.3 (s). ^{13}C{^{1}H} NMR ($CDCl_3$, 25 °C, 75.49 MHz): δ 25.6 (s, THF−O*C*H$_2$); 55.1 (apparent pentet AXX'$_3$, P*C*H$_2$); 68.0 (s, THF−OCH$_2$*C*H$_2$); 116.3 (s, Ph *m*–C); 124.3 (s, Ph *p*–C); 129.2 (s, Ph *o*–C); 149.4 (s, Ph *ipso*–C). Anal. Calcd for $C_{92}H_{100}Mo_4N_{16}NiO_2P_4$ (f.w. 2028.23 g mol^{-1}): C, 54.48; H, 4.97; N, 11.05. Found: C, 46.42 ; H, 4.95 ; N, 10.69. Elemental analyses on multiple samples had appropriate N and H analyses, but suffered from consistently low C values.

Alternate synthesis of 5b. On an NMR scale, a mixture of Ni(acac)$_2$ (5 mg, 0.02 mmol) and **2b** (18 mg, 0.04 mmol, 2 equiv) were dissolved in 1 mL of THF whereupon and immediate colour change to brown was observed. The reaction was monitored by multinuclear NMR spectroscopy. After 30 min, resonances associated with **5b** were observed as the major product. Orange coloured X-ray quality crystals precipitated from the crude reaction mixture overnight in the tube.

Synthesis of Ni[P(CH$_2$N–(CH$_3$)$_2$C$_6$H$_3$)$_3$Mo(*μ*–N)VMes$_3$]$_4$ (6a). Compound **5a** (30 mg, 0.03 mmol, 4 equiv) was dissolved in 0.7 mL of THF and transferred to an NMR tube. The solution was layered with a THF solution (0.2 mL) of VMes$_3$(THF) (2.2 mg, 0.008 mmol), and left undisturbed for weeks. Brown X-ray quality crystals precipitated from solution and were able to

confirm connectivity. Anal. Calcd for $C_{216}H_{264}Mo_4N_{16}NiP_4V_4$ (f.w. 3854.71 g mol^{-1}): C, 67.30; H, 6.90; N, 5.81. Found: C, 60.22 ; H, 6.97 ; N, 6.12 . Similar to **4a**, elemental analyses on multiple samples had appropriate N and H analyses, but suffered from variable and consistently low C values.

X-ray Crystallography. X-ray structures of **2a-c**, **3**, **4a**, **5a**, **5b** and **6a** were obtained at low temperature, with each crystal covered in Paratone and placed rapidly into the cold N_2 stream of the Kryo-Flex low-temperature device. The data were collected using SMART[31] software on a Bruker APEX CCD diffractometer, using a graphite monochromator with Mo Kα radiation (λ = 0.71073 Å). A hemisphere of data was collected using a counting time of 10-30 s per frame. Details of crystal data, data collection, and structure refinement for structures **2a-c**, **3**, **4a**, **5b** and **6a** are listed in Table 1. Data reductions were performed using SAINT[32] software, and the data were corrected for absorption using SADABS.[33] The structures were solved by direct methods using SIR97[34] and refined by full-matrix least-squares on F^2, and anisotropic displacement parameters for the non-H atoms, with the exception of some highly disordered solvent molecules, were determined using SHELX-97[35] and the WinGX[36] software package. Thermal ellipsoid plots were produced using ORTEP32.[37] The structures of **2c**, **5a**, and **6a** are of low quality. Complex **2c** crystallized as poorly diffracting plates, and compound **5a** diffracted poorly and the structure solution was complicated by a large number of disordered cocrystallized THF molecules. Complex **6a** crystallized from the reaction mixture as very large crystals that diffracted poorly. The structure of **6a** suffered from multiple issues, including likely twinning, and a large number of disordered solvent molecules disorder in the void spaces. No adequate solution could be found in any space group. The structure solution essentially thus only provides

evidence of connectivity. CCDC 1058899-1058906 contains the supplementary crystallographic data for this paper.

Acknowledgement is made to the Natural Sciences and Engineering Research Council (NSERC) of Canada for a discovery grant for S.A.J. and a post-graduate scholarship for J.A.H, the facilities of the Shared Hierarachical Academic Research Computing Network (SHARCNET:www.sharcnet.ca) and Compute/Calcul Canada, and Andrew R. Geisheimer and Daniel B. Leznoff for their assistance in the collection of SQUID magnetometer data.

Table 1. Crystallographic data for compounds **2a–b**, **3**, **4a** and **5b**.

	2a	**2b**	**3**	**4a**	**5b**
Empirical Formula	$C_{27}H_{33}MoN_4P$	$C_{21}H_{21}MoN_4P$	$C_{69}H_{58}F_{36}Mo_2N_{12}P_2$	$C_{129}H_{156}Mo_2N_8P_2V_2$	$C_{108}H_{132}Mo_4N_{16}NiO_6P_4$
Formula Weight	540.48	456.33	1993.09	2174.32	2316.65
Crystal System	Monoclinic	Monoclinic	Monoclinic	Monoclinic	Trigonal
a (Å)	10.5565(14)	11.2509(11)	13.272(2)	16.151(3)	24.8542(12)
b (Å)	10.6963(14)	7.2175(7)	18.543(3)	40.821(7)	24.8542(12)
c (Å)	22.4401(30)	24.609(2)	17.109(3)	17.845(3)	29.932(3)
α (degrees)	90.	90.	90.	90.	90.
β (degrees)	95.443(1)	90.894(1)	109.595(2)	99.871(2)	90.
γ (degrees)	90.	90.	90.	90.	120.
V (Å^3)	2522.41(6)	1998.1(3)	3966.8(12)	11591(3)	16012.7(19)
Space Group	$P2_1/c$	$P2_1/n$	$P2_1/c$	$P2_1/n$	$R\bar{3}$
Z value	4	4	2	4	6
D_{calc} (g/cm^3)	1.42	1.517	1.669	1.246	1.441
μ(MoKα) (mm^{-1})	0.606	0.749	0.491	0.447	0.751
Temperature (K)	173(2)	173(2)	173(2)	173(2)	173(2)
$2\theta_{max}$ (degrees)	55.0	55.0	50.0	55.0	55.0
Total No. of Reflns	27304	21425	35984	129151	60145
No. Unique Reflns; R_{int}	5714; 0.048	4522; 0.077	6984; 0.044	26282; 0.047	16009; 0.0423
Transmission Factors	0.98–0.93	0.99–0.87	0.87–0.87	0.92–0.88	0.95–0.87
No. with $I \geq 2\sigma(I)$	4759	3000	5601	20682	14650
No. Variables	304	244	599	1285	835
R; wR_2 (all data)	0.045; 0.089	0.078; 0.105	0.061; 0.131	0.067; 0.115	0.042; 0.08
GOF	1.062	1.01	1.072	1.061	1.055
Residual Density (e$^-$/Å^3)	0.956; −0.519	0.736; −0.584	1.237; −0.646	0.772; −0.435	0.778; −0.332

References:

(1) (a) Ritleng, V.; Chetcuti, M. J. *Chem. Rev.* **2007**, *107*, 797-858; (b) Haak, R. M.; Wezenberg, S. J.; Kleij, A. W. *Chem. Commun.* **2010**, *46*, 2713-2723; (c) Bratko, I.; Gomez, M. *Dalton Trans.* **2013**, *42*, 10664-10681.
(2) (a) Busetto, L.; Maitlis, P. M.; Zanotti, V. *Coord. Chem. Rev.* **2010**, *254*, 470-486; (b) Cooper, B. G.; Napoline, J. W.; Thomas, C. M. *Catal. Rev. Sci. Eng.* **2012**, *54*, 1-40; (c) King, P. J. *Annu. Rep. Prog. Chem., Sect. A Inorg. Chem.* **2008**, *104*, 325-342; (d) Komiya, S. *Coord. Chem. Rev.* **2012**, *256*, 556-573; (e) Mandal, S. K.; Roesky, H. W. *Acc. Chem. Res.* **2010**, *43*, 248-259; (f) Zanotti, V. *Pure Appl. Chem.* **2010**, *82*, 1555-1568.
(3) (a) Han, H.; Elsmaili, M.; Johnson, S. A. *Inorg. Chem.* **2006**, *45*, 7435-7445; (b) Raturi, R.; Lefebvre, J.; Leznoff, D. B.; McGarvey, B. R.; Johnson, S. A. *Chem.--Eur. J.* **2008**, *14*, 721-730.
(4) Hatnean, J. A.; Raturi, R.; Lefebvre, J.; Leznoff, D. B.; Lawes, G.; Johnson, S. A. *J. Am. Chem. Soc.* **2006**, *128*, 14992-14999.
(5) (a) Kuzu, I.; Krummenacher, I.; Meyer, J.; Armbruster, F.; Breher, F. *Dalton Trans.* **2008**, 5836-5865; (b) Armbruster, F.; Fernandez, I.; Breher, F. *Dalton Trans.* **2009**, 5612-5626; (c) Baier, F.; Fei, Z.; Gornitzka, H.; Murso, A.; Neufeld, S.; Pfeiffer, M.; Rudenauer, I.; Steiner, A.; Stey, T.; Stalke, D. *J. Organomet. Chem.* **2002**, *661*, 111-127; (d) Kling, C.; Leusser, D.; Stey, T.; Stalke, D. *Organometallics* **2011**, *30*, 2461-2463; (e) Meinholz, M. M.; Pandey, S. K.; Deuerlein, S. M.; Stalke, D. *Dalton Trans.* **2011**, *40*, 1662-1671; (f) Meinholz, M. M.; Stalke, D. *Z. Anorg. Allg. Chem.* **2011**, *637*, 2233-2238; (g) Objartel, I.; Ott, H.; Stalke, D. *Z. Anorg. Allg. Chem.* **2008**, *634*, 2373-2379; (h) Objartel, I.; Pott, N. A.; John, M.; Stalke, D. *Organometallics* **2010**, *29*, 5670-5675; (i) Stey, T.; Henn, J.; Stalke, D. *Chem. Commun. (Cambridge, U. K.)* **2007**, 413-415; (j) Stey, T.; Pfeiffer, M.; Henn, J.; Pandey, S. K.; Stalke, D. *Chem.--Eur. J.* **2007**, *13*, 3636-3642; (k) Stey, T.; Stalke, D. *Z. Anorg. Allg. Chem.* **2005**, *631*, 2931-2936; (l) Viciano, M.; Sanau, M.; Peris, E. *Organometallics* **2007**, *26*, 6050-6054; (m) Weigand Jan, J.; Feldmann, K.-O.; Echterhoff Antje, K. C.; Ehlers Andreas, W.; Lammertsma, K. *Angew Chem Int Ed Engl* **2010**, *49*, 6178-81; (n) Weigand, J. J.; Feldmann, K.-O.; Echterhoff, A. K. C.; Ehlers, A. W.; Lammertsma, K. *Angew. Chem., Int. Ed.* **2010**, *49*, 6178-6181, S6178/1-S6178/37; (o) Carlson, B.; Aquino, A. J. A.; Hope-Weeks, L. J.; Whittlesey, B.; McNerney, B.; Hase, W. L.; Krempner, C. *Chem. Commun. (Cambridge, U. K.)* **2011**, *47*, 11089-11091; (p) Li, H.; Hope-Weeks, L. J.; Krempner, C. *Chem. Commun. (Cambridge, U. K.)* **2011**, *47*, 4117-4119; (q) Zeckert, K.; Zahn, S.; Kirchner, B. *Chem. Commun.* **2010**, *46*, 2638-2640; (r) Li, H.; Hung-Low, F.; Krempner, C. *Organometallics* **2012**, *31*, 7117-7124; (s) Gonzalez-Gallardo, S.; Kuzu, I.; Ona-Burgos, P.; Wolfer, T.; Wang, C.; Klinkhammer, K. W.; Klopper, W.; Braese, S.; Breher, F. *Organometallics* **2014**, *33*, 941-951; (t) Creutz, S. E.; Krummenacher, I.; Clough, C. R.; Cummins, C. C. *Chem. Sci.* **2011**, *2*, 2166-2172.
(6) Gade, L. H. *Acc. Chem. Res.* **2002**, *35*, 575-582.
(7) (a) Han, H.; Johnson, S. A. *Organometallics* **2006**, *25*, 5594-5602; (b) Han, H.; Johnson, S. A. *Eur. J. Inorg. Chem.* **2008**, 471-482.
(8) Keen, A. L.; Doster, M.; Han, H.; Johnson, S. A. *Chem. Commun.* **2006**, 1221-1223.
(9) (a) Curley, J. J.; Sceats, E. L.; Cummins, C. C. *J. Am. Chem. Soc.* **2006**, *128*, 14036-14037; (b) Johnson, M. J. A.; Lee, P. M.; Odom, A. L.; Davis, W. M.; Cummins, C. C. *Angew. Chem., Int. Ed.* **1997**, *36*, 87-91; (c) Woo, L. K. *Chem. Rev.* **1993**, *93*, 1125-36; (d) Laplaza, C. E.; Johnson, A. R.; Cummins, C. C. *J. Am. Chem. Soc.* **1996**, *118*, 709-10.

(10) (a) Gdula, R. L.; Johnson, M. J. A. *J. Am. Chem. Soc.* **2006**, *128*, 9614-9615; (b) Geyer, A. M.; Gdula, R. L.; Wiedner, E. S.; Johnson, M. J. A. *J. Am. Chem. Soc.* **2007**, *129*, 3800-3801; (c) Wiedner, E. S.; Gallagher, K. J.; Johnson, M. J. A.; Kampf, J. W. *Inorg. Chem.* **2011**, *50*, 5936-5945.
(11) (a) Christian, G.; Stranger, R.; Yates, B. F.; Cummins, C. C. *Dalton Trans.* **2007**, 1939-1947; (b) Cummins, C. C. *Chem. Commun.* **1998**, 1777-1786; (c) Curley, J. J.; Cook, T. R.; Reece, S. Y.; Muller, P.; Cummins, C. C. *J. Am. Chem. Soc.* **2008**, *130*, 9394-9405; (d) Laplaza, C. E.; Johnson, M. J. A.; Peters, J.; Odom, A. L.; Kim, E.; Cummins, C. C.; George, G. N.; Pickering, I. J. *J. Am. Chem. Soc.* **1996**, *118*, 8623-8638.
(12) Chen, S.; Chisholm, M. H.; Davidson, E. R.; English, J. B.; Lichtenberger, D. L. *Inorg. Chem.* **2009**, *48*, 828-837.
(13) Sceats, E. L.; Figueroa, J. S.; Cummins, C. C.; Loening, N. M.; Van der Wel, P.; Griffin, R. G. *Polyhedron* **2004**, *23*, 2751-2768.
(14) (a) Figueroa, J. S.; Piro, N. A.; Clough, C. R.; Cummins, C. C. *J. Am. Chem. Soc.* **2006**, *128*, 940-950; (b) Gebeyehu, Z.; Weller, F.; Neumueller, B.; Dehnicke, K. *Z. Anorg. Allg. Chem.* **1991**, *593*, 99-110; (c) Tsai, Y.-C.; Johnson, M. J. A.; Mindiola, D. J.; Cummins, C. C.; Klooster, W. T.; Koetzle, T. F. *J. Am. Chem. Soc.* **1999**, *121*, 10426-10427.
(15) (a) Kerby, M. C.; Eichhorn, B. W.; Creighton, J. A.; Vollhardt, K. P. C. *Inorg. Chem.* **1990**, *29*, 1319-23; (b) Girolami, G. S.; Andersen, R. A. *Inorg. Chem.* **1982**, *21*, 1318-21.
(16) Wampler, K. M.; Schrock, R. R. *Inorg. Chem.* **2007**, *46*, 8463-8465.
(17) Poater, A.; Cosenza, B.; Correa, A.; Giudice, S.; Ragone, F.; Scarano, V.; Cavallo, L. *Eur. J. Inorg. Chem.* **2009**, 1759-1766.
(18) Clavier, H.; Nolan, S. P. *Chem. Commun.* **2010**, *46*, 841-861.
(19) WinDNMR, NMR spectrum calculations; Hans J. Reich: Madison, WI, 2005.
(20) Chisholm, M. H.; Delbridge, E. E.; Kidwell, A. R.; Quinlan, K. B. *Chem. Commun.* **2003**, 126-127.
(21) (a) Agapie, T.; Odom, A. L.; Cummins, C. C. *Inorg. Chem.* **2000**, *39*, 174-179; (b) Seymore, S. B.; Brown, S. N. *Inorg. Chem.* **2002**, *41*, 462-469.
(22) Dubberley, S. R.; Tyrrell, B. R.; Mountford, P. *Acta Crystallogr., Sect. C Cryst. Struct. Commun.* **2001**, *C57*, 902-904.
(23) Song, J.-I.; Gambarotta, S. *Chem.--Eur. J.* **1996**, *2*, 1258-1263.
(24) (a) Vivanco, M.; Ruiz, J.; Floriani, C.; Chiesi-Villa, A.; Rizzoli, C. *Organometallics* **1993**, *12*, 1802-10; (b) Weber, K.; Korn, K.; Schorm, A.; Kipke, J.; Lemke, M.; Khvorost, A.; Harms, K.; Sundermeyer, J. *Z. Anorg. Allg. Chem.* **2003**, *629*, 744-754.
(25) Greco, G. E.; O'Donoghue, M. B.; Seidel, S. W.; Davis, W. M.; Schrock, R. R. *Organometallics* **2000**, *19*, 1132-1149.
(26) Ananikov, V. P.; Gayduk, K.; Starikova, Z. A.; Beletskaya, I. P. *Organometallics* **2010**, *29*, 5098-5102.
(27) (a) Darensbourg, D. J.; Decuir, T. J.; Stafford, N. W.; Robertson, J. B.; Draper, J. D.; Reibenspies, J. H.; Katho, A.; Joo, F. *Inorg. Chem.* **1997**, *36*, 4218-4226; (b) Hursthouse, M. B.; Izod, K. J.; Motevalli, M.; Thornton, P. *Polyhedron* **1994**, *13*, 151-3; (c) Kourkine, I. V.; Maslennikov, S. V.; Ditchfield, R.; Glueck, D. S.; Yap, G. P. A.; Liable-Sands, L. M.; Rheingold, A. L. *Inorg. Chem.* **1996**, *35*, 6708-6716; (d) Kuhl, O.; Junk, P. C.; Hey-Hawkins, E. *Z. Anorg. Allg. Chem.* **2000**, *626*, 1591-1594; (e) Langer, J.; Goels, H.; Gillies, G.; Walther, D. *Z. Anorg. Allg. Chem.* **2005**, *631*, 2719-2726.

(28) Pangborn, A. B.; Giardello, M. A.; Grubbs, R. H.; Rosen, R. K.; Timmers, F. J. *Organometallics* **1996**, *15*, 1518-20.
(29) Vivanco, M.; Ruiz, J.; Floriani, C.; Chiesi-Villa, A.; Rizzoli, C. *Organometallics* **1993**, *12*, 1794-801.
(30) Krysan, D. J.; Mackenzie, P. B. *J. Org. Chem.* **1990**, *55*, 4229-30.
(31) SMART, Molecular analysis research tool; Bruker AXS Inc. Madison, WI,:2001. .
(32) SAINTPlus, Data reduction and correction program; Bruker AXS Inc.: Madison, WI, 2001.
(33) SADABS, An empirical absorption correction program; Bruker AXS Inc.: Madison, WI, 2001.
(34) Altomare, A.; Burla, M. C.; Camalli, M.; Cascarano, G. L.; Giacovazzo, C.; Guagliardi, A.; Moliterni, A. G. G.; Polidori, G.; Spagna, R. *J. Appl. Crystallogr.* **1999**, *32*, 115-119.
(35) Sheldrick, G. M. SHELXL-97; Universitat Gottingen: Gottingen, 1997.
(36) Farrugia, L. J. *J. Appl. Crystallogr.* **1999**, *32*, 837-838.
(37) Farrugia, L. J. *J. Appl. Crystallogr.* **1997**, *30*, 565.